Viscoelastic Registration of Medical Images

Zhao Yi Justin Wan

Abstract

Since the physical behavior of many tissues is shown to be viscoelastic, we propose a novel registration technique for medical images via physical principles of viscoelasticity. It allows the template and the target images to differ by large local deformations like viscous fluid and small local deformations like elastic solid. With an extra elastic term introduced, the proposed model constrains the transformation by coupled viscoelastic behavior and therefore reduces the smearing effect caused by the fluid terms. We apply our approach to both artificial test data and MR brain slices yielding accurate registration results.

1 Introduction

Numerous algorithms have been explored in nonrigid registration area [15] to capture variabilities of biological structures accross individuals and at different times. Broit [3] was the first to study this problem using physically based models. In his approach the transformation process was modeled by deformations of an elastic solid. This approach was extended by Bajcsy et al. [1] and various variational forms [4, 8] were proposed later. Limited by the constraint of linear elasticity, the elastic model can only accommodate locally small deformations. To overcome this drawback, Christensen et al. [7] introduced another approach which modeled the transformation process by a viscous fluid flow. The fluid model can allow locally large deformations, but it tends to smear images because of the fluid viscosity.

The regions of interest in medical images are usually tissues, such as brain, corona, and ventricle. If the change of the regions is caused by the behavior of the corresponding biophysical structures, it is quite straight forward and reasonable to acquire the transformation by simulating the deformation as a physical process. Since most tissues behave between elastic solid and viscous fluid [13], either an elastic approach or a fluid approach itself may not be accurate for registration modeling. Our idea is to develop a combined viscoelastic approach which has the property of both elastic solid and viscous fluid to achieve better registration.

In this paper, we present a novel viscoelastic registration technique expressed in a fluid framework. It allows an image pair to differ by large deformations like viscous fluid and small deformations like elastic solid. The basic idea in this technique is to let the template image transform by simulating the deformation process as a viscoelastic fluid flow to the target image. By introducing an extra elastic term, the proposed model constrains the transformation by coupled viscoelastic behavior and therefore decreases the blurring effect caused by the fluid terms. The resulting partial differential equations are nonlinear elliptic-hyperbolic equations of vector form whose solution describes the coordinate transformation between the template and the target images. It can be numerically solved using finite difference method. We have successfully applied the transformation model to medical images yielding fast and accurate registrations.

A similar approach was proposed by Tang et al. [16]. However, they simplied the linear Maxwell model by linear addition of fluid part (dashpot) and elastic part (spring), and solved for each part separately. Such simplification is not quite right since for viscoelastic matter those two parts are supposed to be coupled together. Our model correctly applies the coupled constitutive law and thus obtain a more realistic meaning in medical imaging.

The rest of the paper is organized as follows. Section 2 contains an overview of the linear Maxwell model for viscoelastic fluid flow, followed by the proposed formulation of the image registration problem in Section 3. Section 4 presents a complete numerical algorithm for solving the consequent modified Navier's equation. Section 5 shows experimental results of this approach on 2D sythetic/real images. Finally, conclusions are drawn in Section 6.

2 Viscoelastic Fluid

We consider the template image as a compressible fluid. The external force applied to the continuum is balanced by the internal force caused by the resulting deformation. The conservation of momentum equation can be written as

$$\nabla \cdot \mathcal{T} + \mathbf{f} - \nabla p = \rho(\frac{\partial \mathbf{u}}{\partial t} + (\mathbf{u} \cdot \nabla)\mathbf{u}), \tag{1}$$

where $\mathcal{T}$ is the extra stress tensor, $\mathbf{f}$ is the external force and will be defined later by information from the template and the target images, ρ is the density of fluid which is assumed to be constant here, $\mathbf{u}$ is the velocity field, and p is the pressure. The right side of equation (1) represents the force of inertia, i.e., the density times the acceleration of fluid.

A simplified model is obtained [11] for very low Reynold's number flow where the pressure gradient ∇p and the inertial term $\rho(\frac{\partial \mathbf{u}}{\partial t} + (\mathbf{u} \cdot \nabla)\mathbf{u})$ are neglected, such that (1) becomes

$$\nabla \cdot \mathcal{T} + \mathbf{f} = 0. \tag{2}$$

The extra stress tensor $\mathcal{T}$ represents the force which the material develops in response to being deformed. To complete the mathematical formulation, we need a constitutive law relating $\mathcal{T}$ to the motion.

The constitutive law for a Newtonian fluid [9] models the extra stress tensor $\mathcal{T}$ by

$$\mathcal{T} = \lambda tr(\mathcal{D})\mathcal{I} + 2\mu\mathcal{D}, \tag{3}$$

where λ and μ are the viscosity constants, $\mathcal{D} = \frac{1}{2}(\nabla \mathbf{u} + (\nabla \mathbf{u})^T)$ is the rate of deformation tensor, and $\mathcal{I}$ is the identity tensor. In order to capture the elastic behavior in the transformation, we model the fluid as a viscoelastic fluid [14]. The stress depends not only on the current motion of the fluid, but also on the history of the motion. If we assume that this dependence is linear, the extra stress tensor given by the Maxwell theory of linear viscoelasticity satisfies

$$\mathcal{T}_t + \beta \mathcal{T} = \lambda tr(\mathcal{D})\mathcal{I} + 2\mu\mathcal{D}. \tag{4}$$

Here β is a constant, the quantity $\frac{1}{\beta}$ has the dimension of time and is known as a relaxation time [14]. It is, roughly speaking, a measure of the time for which the fluid remembers the flow history. The behavior of viscoelastic fluids depend crucially on how this time scale relates to other time scales relevant to the flow. The ratio of a time scale for the fluid memory to a time scale of the flow is an important dimensionless measure of the importance of elasticity.

The equations (2) and (4) for a viscoelastic fluid are coupled together, we have to reformulate the mixed system in a way that tries to separate the motion from the constitutive law. Thus, we split the extra tensor term to an ordinary compressible fluid part plus an elastic part

$$\mathcal{T} = \lambda tr(\mathcal{D})\mathcal{I} + 2\mu\mathcal{D} + \mathcal{E}, \tag{5}$$

where $\mathcal{E}$ is the elastic tensor. This is known as the elastic-viscous stress-splitting (EVSS) method [10]. Substitute (5) into (2) we obtain

$$\mu \triangle \mathbf{u} + (\mu + \lambda)\nabla(\nabla \cdot \mathbf{u}) + \nabla \cdot \mathcal{E} + \mathbf{f} = 0, \tag{6}$$

where $\triangle$ is the Laplacian operator, ∇ is the gradient operator, and $\nabla\cdot$ is the divergence operator. This is the main PDE we are solving for viscoelastic registration. It is an extension for the Newtonian fluid case where $\mathcal{E} = \mathbf{0}$ and the momentum equation (6) assumes the usual Navier-Stokes form

$$\mu \triangle \mathbf{u} + (\mu + \lambda)\nabla(\nabla \cdot \mathbf{u}) + +\mathbf{f} = 0. \tag{7}$$

3 Registration Formulation

We define the template image as $I_1(\mathbf{x})$ and the target image as $I_2(\mathbf{x})$, where $0 \leq I_1(\mathbf{x}), I_2(\mathbf{x}) \leq 1$, and $\mathbf{x} \in \Omega$ is the image region. The purpose of the registration is to determine a coordinate transformation $\mathbf{r}(\mathbf{x})$ of $I_1(\mathbf{x})$ onto $I_2(\mathbf{x})$ such that $I_1(\mathbf{x} - \mathbf{r}(\mathbf{x}))$ will be small in some measure M. Therefore the registration can also be stated as a minimization problem

$$\min_{\mathbf{r}(\mathbf{x})} M(I_1(\mathbf{x}), I_2(\mathbf{x}), \mathbf{r}(\mathbf{x})). \tag{8}$$

The force field $\mathbf{f}(\mathbf{x}, \mathbf{r}(\mathbf{x}))$ is used to drive the flow from image $I_1(\mathbf{x})$ to image $I_2(\mathbf{x})$. It is defined as the derivative of any matching criteria M on the image pair. Here we use a Gaussian sensor model [5] to induce the matching criteria:

$$M(I_1(\mathbf{x}), I_2(\mathbf{x}), \mathbf{r}(\mathbf{x}, t)) = \frac{\alpha}{2} \int_{\Omega} \|I_1(\mathbf{x} - \mathbf{r}(\mathbf{x}, t)) - I_2(\mathbf{x})\|^2 d\mathbf{x}, \tag{9}$$

where α is a parameter. Taking the variation of this cost function with respect to displacement, $\mathbf{r}(\mathbf{x}, t)$, gives the force field

$$\mathbf{f}(\mathbf{x}, \mathbf{r}(\mathbf{x}, t)) = \alpha(I_1(\mathbf{x} - \mathbf{r}(\mathbf{x}, t)) - I_2(\mathbf{x}))\nabla I_1(\mathbf{x} - \mathbf{r}(\mathbf{x}, t)). \tag{10}$$

We use an Eulerian reference frame to update movement of the viscoelastic fluid in the image. The displacement field $\mathbf{r}(\mathbf{x})$ and velocity filed $\mathbf{u}(\mathbf{x})$ are both defined based on spatial positions. Consequently, we use a fixed spatial grid to track the deformation. Since $\mathbf{u}(\mathbf{x}, t)$ and $\mathbf{r}(\mathbf{x}, t)$ describe the velocity and the displacement of fluid as it move through $\mathbf{x}$ at time t, we have the following relationship

$$\mathbf{u}(\mathbf{x}, t) = \frac{\partial \mathbf{r}(\mathbf{x}, t)}{\partial t} + \nabla \mathbf{r}(\mathbf{x}, t)\mathbf{u}(\mathbf{x}, t). \tag{11}$$

Combining equations (4), (5), (6), (10), and (11), the viscoelastic registration model requires solving the following PDE system

$$\begin{aligned}
&\mu \triangle \mathbf{u}(\mathbf{x}, t) + (\lambda + \mu)\nabla(\nabla \cdot \mathbf{u})(\mathbf{x}, t) + \nabla \cdot \mathcal{E} + \mathbf{f}(\mathbf{x}, \mathbf{r}(\mathbf{x}, t)) = 0,\\
&\frac{\partial \mathbf{r}(\mathbf{x}, t)}{\partial t} = \mathbf{u}(\mathbf{x}, t) - \nabla \mathbf{r}(\mathbf{x}, t)\mathbf{u}(\mathbf{x}, t),\\
&\frac{\partial \mathcal{T}(\mathbf{x}, t)}{\partial t} = -\beta \mathcal{T}(\mathbf{x}, t) + \mu \Delta \mathbf{u}(\mathbf{x}, t) + (\mu + \lambda)\nabla(\nabla \cdot \mathbf{u}(\mathbf{x}, t)),\\
&\mathcal{E}(\mathbf{x}, t) = \mathcal{T}(\mathbf{x}, t) - \mu \Delta \mathbf{u}(\mathbf{x}, t) - (\mu + \lambda)\nabla(\nabla \cdot \mathbf{u}(\mathbf{x}, t)),\\
&\mathbf{f}(\mathbf{x}, \mathbf{r}(\mathbf{x}, t)) = \alpha(I_1(\mathbf{x} - \mathbf{r}(\mathbf{x}, t)) - I_2(\mathbf{x}))\nabla I_1(\mathbf{x} - \mathbf{r}(\mathbf{x}, t)),
\end{aligned}$$

which includes nonlinearity introduced by the external force and the kinematic derivatives.

4 Implementation

Because the gradient operator is sensitive to the noise in the image, we convolve the deformed template $I_1(\mathbf{x} - \mathbf{r}(\mathbf{x}, t))$ with a Gaussian kernel prior to the gradient computation. This leads equation (10) to the following

$$\mathbf{f}(\mathbf{x}, \mathbf{r}(\mathbf{x}, t)) = \alpha(I_1(\mathbf{x} - \mathbf{r}(\mathbf{x}, t)) - I_2(\mathbf{x}))\nabla(G_\sigma * I_1(\mathbf{x} - \mathbf{r}(\mathbf{x}, t))), \tag{12}$$

where G_σ denotes the Gaussian kernel with standard deviation of σ and $*$ is the convolution operator.

To update movement of fluid through time, we discretize time domain $[0, +\infty]$ into small intervals $0 = t_0 < t_1 < \ldots < t_n < t_{n+1} < \ldots$ and apply Euler explicit integration over time. The discretized time formula is given by

$$\mathcal{T}^{n+1}(\mathbf{x}) = (1 - \beta \Delta t)\mathcal{T}^n(\mathbf{x}) + \Delta t(\mu \Delta \mathbf{u}^n(\mathbf{x}) + (\lambda + \mu)\nabla(\nabla \cdot \mathbf{u}^n(\mathbf{x}))), \tag{13}$$

$$\mathbf{r}^{n+1}(\mathbf{x}) = \mathbf{r}^n(\mathbf{x}) + \Delta t(\mathcal{I} - \nabla \mathbf{r}^n(\mathbf{x}))\mathbf{u}^n(\mathbf{x}), \tag{14}$$

where

$\mathcal{T}^{n+1}(\mathbf{x}) \approx \mathcal{T}(\mathbf{x}, t_{n+1})$ is the approximation of extra stress tensor field at time t_{n+1},
$\mathbf{u}^{n+1}(\mathbf{x}) \approx \mathbf{u}(\mathbf{x}, t_{n+1})$ is the approximation of velocity field at time t_{n+1},
$\mathbf{r}^{n+1}(\mathbf{x}) \approx \mathbf{r}(\mathbf{x}, t_{n+1})$ is the approximation of displacement field at time t_{n+1},
$\Delta t = t_{n+1} - t_n$ is the time interval.

We need Δt to be small enough for stable Euler explicit integration. Thus we introduce a threshold d_{max} [2] for displacement per timestep such that $\Delta t(\mathcal{I} - \nabla \mathbf{r}(\mathbf{x}, t))\mathbf{u}(\mathbf{x}, t) < d_{max}$. Besides, We require the Jacobian $J = \|\mathcal{I} - \nabla \mathbf{r}^n\|$ [7] greater than zero in order to obtain a regular transformation. The complete algorithm for solving the viscoelastic registration problem consequently becomes

1. Initialize $\mathbf{u}^0(\mathbf{x}) = \mathbf{0}$, $\mathbf{r}^0(\mathbf{x}) = \mathbf{0}$, and $\mathcal{T}^0(\mathbf{x}) = \mathcal{I}$.

2. Calculate the external force $\mathbf{f}^n(\mathbf{x})$ at time t_n using equation (11).

3. If $\mathbf{f}^n(\mathbf{x})$ is below a stopping criteria for all $\mathbf{x}$ or the maximum number of iterations is reached, STOP.

4. Calculate the extra stress tensor $\mathcal{T}^n(\mathbf{x})$ at time t_n using equation (13).

5. Calculate the elastic tensor $\mathcal{E}^n(\mathbf{x})$ at time t_n using equation (5).

6. Solve equation (6) by SOR [6] for instantaneous velocity $\mathbf{u}^n(\mathbf{x})$ under fixed force $\mathbf{f}^n(\mathbf{x})$ at time t_n.

7. Choose $\Delta t < d_{max}/(\mathcal{I} - \nabla \mathbf{r}^n(\mathbf{x}))\mathbf{u}^n(\mathbf{x})$, to perform Euler explicit integration using equation (14).

8. If the Jacobian $J = \|\mathcal{I} - \nabla \mathbf{r}^n(\mathbf{x})\|$ is less than 0.5, regrid the template.

9. $n = n + 1$, GOTO step 2.

5 Results

The proposed approach is implemented in C and executed at a desktop PC of P4 2.8GHz with 1GB memory. The parameters are set to $m = 1$ and $\alpha = 100$. The maximum number of iterations is set to 250 and the stopping criteria is set to 0.01. We have applied the proposed algorithm to three experiments. Four sets of images are presented for each registration: 1. template image; 2. target image; 3. transformed image after registration; 4. difference image between transformed image and target image.

The first experiment is designed to demonstrate that our model can accommodate large deformation like fluid algorithm as well as achieving a similar

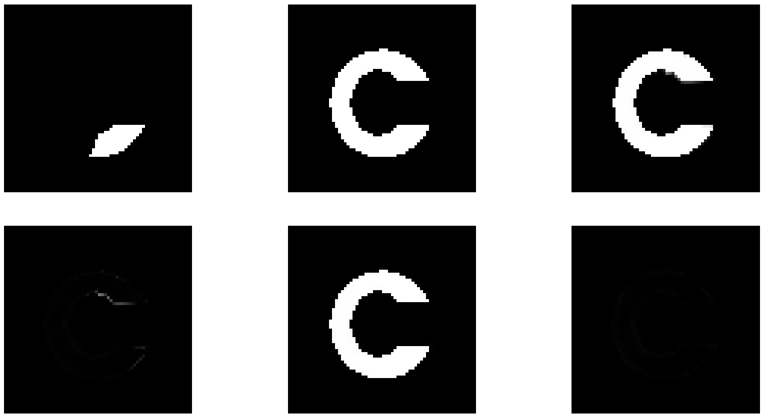

Figure 1: qualitative results of experiment 1. From left to right, top to bottom: (a)template image; (b)target image; (c)transformed image obtained by fluid model; (d)difference image between (b) and (c); (e)transformed image obtained by proposed model; (f)difference image between (b) and (f).

displacement map. The test data is a synthetic image with size 64×64 pixels which is similar to the image used by [7]. The results are shown in Figure 1 with comparison to fluid model. Besides the four sets of images mentioned above, we include the displacement map as well. It is what we desire that the transformed image is almost the same as the target image, and the displacement map is largely curved from a small patch to the whole letter "C".

The second experiment is designed to demonstrate that our model can decrease the smearing artifacts caused by fluid approach. The test data is a synthetic image with size 128×128 pixels which is similar to the image used by [12]. The results are shown in Figure 2 with comparison to fluid model. From the difference images, we can see clearly that the proposed model achieve a transformed image with sharper edges than the fluid approach. Thus, the blurring effect introduced by the viscosity term is successfully bounded by the extra elastic term.

The third experiment is designed to demonstrate that our model can capture complex transformation in medical images. The test data is an MRI image of human brain with size 256×256 pixels. The results are shown in Figure 3. We can see that the proposed model has successfully registered the template image towards the target image.

To further assess the quality of the registration in the above experiments, mean and variance of the squared sum of intensity difference (SSD), and correlation coefficient (CC) have been calculated and are listed in Table 1.

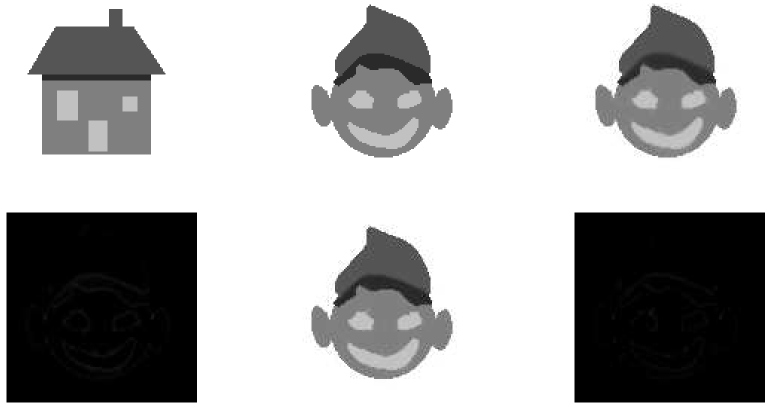

Figure 2: qualitative results of experiment 2. From left to right, top to bottom: (a)template image; (b)target image; (c)transformed image obtained by fluid model; (d)difference image between (b) and (c); (e)transformed image obtained by proposed model; (f)difference image between (b) and (f).

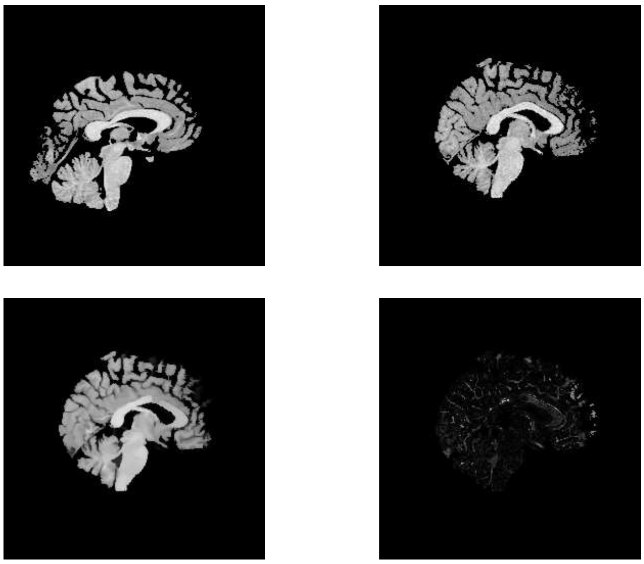

Figure 3: qualitative results of experiment 3. From left to right, top to bottom: (a)template image; (b)target image; (c)transformed image obtained by proposed model; (d)difference image between (b) and (c).

Experiment 1	Mean(SSD)	Var(SSD)	CC
No registration	0.103760	0.092994	0.447277
Fluid	0.000271	0.000027	0.998853
Proposed	0.000015	0.000000	0.999958
Experiment 2	Mean(SSD)	Var(SSD)	CC
No registration	0.046775	0.013727	0.705199
Fluid	0.000154	0.000000	0.999049
Proposed	0.000072	0.000000	0.999545
Experiment 3	Mean(SSD)	Var(SSD)	CC
No registration	0.054380	0.021933	0.523169
Fluid	0.002417	0.000278	0.977904
Proposed	0.002139	0.000269	0.980353

Table 1: qualitative measures for 3 experiments

6 Conclusions

Based on the fact that mechanical behavior of most tissues turns out to be viscoelastic, we propose a novel registration technique for medical images using Maxwell's theory of linear viscoelasticity. The basic idea is to simulate the image deformation process as a viscoelastic fluid flow from the template to the target. The combined viscoelastic model can successfully capture small deformations caused by elastic behaviors as well as large deformations caused by fluid behaviors. Also, the blurring effect is decreased in the proposed model because the viscosity term, which tends to smear images, is bounded by the extra elastic term. Finally, we demonstrate the performance of our approach with comparison to fluid model on synthetic and real images. Future work will be focused on two issues: more efficient numerical algorithms and nonlinear viscoelastic estimation of image deformations.

References

[1] R. Bajcsy and S. Kovacic. Multiresolution elastic matching. *Computer Vision, Graphics, and Image Processing*, 46:1–21, 1989.

[2] M. Bro-Nielsen and C. Gramkow. Fast fluid registration of medical images. In *Proc. Visualization in Biomedical Computing*, pages 267–276, 1996.

[3] C. Broit. *Optimal registration of deformed images.* PhD thesis, University of Pennsylvania, 1981.

[4] G.E. Christensen, S.C. Joshi, and M.I. Miller. Volumetric transformation of brain anatomy. *IEEE Trans. Medical Imaging*, 16:864–877, 1997.

[5] G.E. Christensen, R.D. Rabbitt, and M.I. Miller. A deformable neuroanatomy textbook based on viscous fluid mechanics. In *Proc. Information Science and Systems*, pages 211–216, 1993.

[6] G.E. Christensen, R.D. Rabbitt, and M.I. Miller. 3d brain mapping using a deformable neuroanatomy. *Physics in Medicine and Biology*, 39:609–618, 1994.

[7] G.E. Christensen, R.D. Rabbitt, and M.I. Miller. Deformable templates using large deformation kinematics. *IEEE Trans. Image Processing*, 5:1435–1447, 1996.

[8] C. Davatzikos. Spatial transformation and registration of brain images using elastically deformable models. *Computer Vision and Image Understanding*, 66:207–222, 1997.

[9] M. Griebel, T. Dornseifer, and T. Neunhoeffer. *Numerical Simulation in Fluid Dynamics: A Practical Introduction.* SIAM, 1997.

[10] R. Guenette and M. Fortin. A new mixed finite element method for computing viscoelastic flows. *Non-Newonian Fluid Mechanics*, 60:27–52, 1999.

[11] L.D. Landau and E.M. Lifshitz. *Fluid Mechanics.* Pergamon, 1987.

[12] H. Lester, S.R. Arridge, K.M. Jansons, L. Lemieux, J.V. Hajnal, and A. Oatridge. Nonlinear registration with the variable viscosity fluid algorithm. In *Proc. Information Processing in Medical Imaging*, pages 238–251, 1999.

[13] K. Miller. Finite deformation, linear and nonlinear viscoelastic models of brain tissue mechanical properties. In *Proc. Bioengineering*, 1995.

[14] M. Renardy. *Mathematical Analysis of Viscoelastic Flows.* SIAM, 2000.

[15] D. Ruechert. Nonrigid registration: techniques and applications. *Medical Image Registration*, 13:281–302, 2001.

[16] S. Tang and T. Jiang. Nonrigid registration of medical image by maxwell model of viscoelasticity. *IEEE Symp. Biomedical Imaging: From Nano to Macro*, pages 1443–1446, 2004.